HHS Public Access

Author manuscript

Cancer Cytopathol. Author manuscript; available in PMC 2023 January 01.

Published in final edited form as:

Cancer Cytopathol. 2022 January ; 130(1): 55–71. doi:10.1002/cncy.22502.

Cytologic Features of Sex-cord Stromal Tumors in Women

Liz N. Edmund, MD[1], **Abeer M. Salama, MD**[1], **Rajmohan Murali, MBBS, MD, FRCPA**[1]

[1]Department of Pathology, Memorial Sloan Kettering Cancer Center, New York, New York, NY 10065, USA

Abstract

Background: Gynecologic sex cord-stromal tumors (SCSTs) arise from sex cords of the embryonic gonad and may display malignant behavior. Here we describe the cytomorphologic features of SCSTs in females, including adult and juvenile granulosa cell tumors (AGCTs and JGCTs), Sertoli-Leydig cell tumors (SLCTs) and steroid cell tumor (SCT).

Methods: Available cytology slides from females with a histologic diagnosis of sex-cord stromal tumor between 2009 and 2020 were retrieved from institutional archives and were reviewed with respect to cytoarchitectural features.

Results: There were 25, 2, 2 and 1 cytology specimens from 19, 2, 2 and 1 patients (aged 7–90 years, median 57 years) with AGCT, JGCT, SLCT and SCT, respectively. Features common to all SCSTs included 3-dimensional groups, rosettes, rare papillary fragments, abundant single cells and naked nuclei. Rosettes and a streaming appearance of cell groups were only seen in AGCTs, which also rarely featured eosinophilic hyaline globules and metachromatic stroma. AGCTs exhibited high nuclear:cytoplasmic (N:C) ratios, with mild nuclear pleomorphism, uniform nuclei with finely granular chromatin, nuclear grooves and small nucleoli; in contrast, other SCSTs lacked rosettes and nuclear grooves and had generally lower N:C ratios, greater nuclear pleomorphism, coarse chromatin and more abundant cytoplasm. Mitotic figures, necrosis and inflammation were rarely identified.

Conclusion: AGCTs show cytomorphologic features which are distinct from those of other SCSTs. Careful evaluation of the cytological features and ancillary studies (e.g., immunochemistry for FOXL2, inhibin and calretinin or sequencing for *FOXL2* mutations) can aid in accurate diagnosis of these tumors.

Précis:

Adult granulosa cell tumors show cytomorphologic features which are distinct from those of other types of sex cord-stromal tumor, including microfollicular structures, eosinophilic hyaline globules and longitudinal nuclear grooves in tumor cells. Careful evaluation of the cytologic features and ancillary studies (e.g., immunochemistry for FOXL2, inhibin and calretinin or sequencing for *FOXL2* mutations) can aid in accurate diagnosis of these tumors.

Corresponding author: Rajmohan Murali, MBBS, MD, FRCPA, Department of Pathology, Memorial Sloan Kettering Cancer Center, 1275 York Avenue, New York, NY 10065, Tel: +1-212-639-5905, MuraliR@mskcc.org.

Author contributions: Conceptualization and Methodology (RM); Investigation and Formal Analysis (LNE, AMS, RM); Writing – original draft (LNE); Visualization (LNE, AMS); Writing - Review & Editing (RM, LNE, AMS); Supervision and Project Administration (RM)

Conflict of interest Statement: There are no conflicts of interest.

Keywords

Adult granulosa cell tumor; Granulosa cell tumor; Juvenile granulosa cell tumor; Sertoli-Leydig cell tumor; Sex cord-stromal tumor; Steroid cell tumor

INTRODUCTION

Gynecologic sex cord-stromal tumors (SCSTs) are a heterogeneous group of tumors that arise from the primordial cortex of the embryonic ovary. They account for ~7% of all primary ovarian tumors[1, 2] and occur in both adult and pediatric age groups. They typically present with abdominal pain and manifestations due to overproduction of sex hormones. Acute abdomen due to tumor rupture and hemoperitoneum may occur in about 10% of cases[3].

Granulosa cell tumors are pure sex cord tumors derived from the granulosa cell layer of ovarian follicles and include two subtypes: adult granulosa cell tumors (AGCTs, 95%) and juvenile granulosa cell tumors (JGCTs, 5%). AGCTs constitute 2% of all ovarian malignancies[4–6] and 85% of malignant SCSTs[7]. They occur primarily in perimenopausal women, with a peak between 50 and 55 years of age[8, 9], but can occur in any age group. AGCTs usually present with abdominal pain and abnormal uterine bleeding. They are often associated with endometrial abnormalities due to estrogen excess and overstimulation of the endometrium, including endometrial hyperplasia and endometrial cancer[10]. Serum levels of β-inhibin may be elevated in some patients. These low-grade malignant tumors are usually confined to the ovary at presentation[11], with most cases following a benign clinical course. However, ~20%[4, 12] of AGCTs display overtly malignant behavior, with peritoneal and distant metastases and recurrences in body fluids. Therefore, cytology can play an important role in diagnosis, staging and detection of recurrent disease in these patients.

Histologically, AGCTs are characterized by bland cuboidal to epithelioid cells with scant pale cytoplasm and angulated nuclei with grooves (so-called “coffee bean” nuclei), arranged in various admixtures of architectural patterns including solid nests, cords, trabeculae and diffuse sheets. Microfollicular structures with central eosinophilic material (Call-Exner bodies) are also often seen in these tumors. Immunohistochemically, AGCTs typically express α-inhibin, calretinin, pancytokeratin and WT1.[13] FOXL2 shows strong diffuse nuclear staining in virtually all AGCTs[14]. FOXL2 expression is not specific to AGCTs and can be seen in other SCSTs. Almost all AGCTs harbor the canonical *FOXL2* C134W mutation, which is highly sensitive and specific to this tumor type and is virtually absent in other SCSTs[15, 16]. Several SCST types bear some histologic and immunophenotypic similarities to AGCTs[13, 14, 17] and this may present a diagnostic dilemma in the evaluation of these tumors in cytologic specimens.

Although cytologic features of SCSTs have been previously described in the literature, they are limited to small case series and/or case reports[5, 18–21]. Among the few reported studies, only one cytological preparation (i.e. fine-needle biopsy, FNB) was used to describe the morphology[6, 9, 22]. In this study, we describe the cytomorphologic features, in a variety of

sample types, of a large cohort of AGCTs and compare them to those seen in other types of SCST.

METHODS

This study was conducted with Memorial Sloan Kettering Cancer Center (MSK) institutional research review board approval (protocol #17–634). A retrospective search of MSK databases was conducted to identify all cytology cases from women with a histologic diagnosis of sex-cord stromal tumor, diagnosed between 2009 and 2020. Available cytologic material for each case, including glass slides and digital images, was retrieved from our institutional archives and independently reviewed by three cytopathologists (LE, AS and RM). Salient cytomorphologic features and architectural patterns (detailed in Table 1) were assessed for each case and consensus was reached by all three pathologists. Histologic correlation with the corresponding surgical pathology material was also performed.

RESULTS

There were 30 cytology specimens from 24 females, aged 7–90 years (median 57 years) at diagnosis (Table 2). They included 25 AGCTs from 19 patients, 2 JGCTs from 2 patients, 2 Sertoli Leydig cell tumors (SLCTs) from 2 patients and 1 steroid cell tumor (SCT). The cohort included specimen types from several anatomic sites, including FNB, touch imprints of core biopsies, body cavity fluids, ureteric brushings and peritoneal washings (Table 3). Immunostained slides were available for a small number of cases with cell block material (Table 4).

Specimen cellularity was related to the nature of the specimen, with FNBs and touch imprints having intermediate to high cellularity, while body fluids and washings showed intermediate to low cellularity.

Adult granulosa cell tumors (n=25)

Twenty-three (92%) of 25 specimens from 17 of 19 patients (89%) with AGCT represented recurrent disease. Of the 17 patients with recurrent tumors in cytology, 14 (82%) were staged as FIGO I-II at time of initial diagnosis, with median age of 43 years and a median time to first recurrence of 7.5 years (Table 2). The cytologic specimens reviewed comprised 15 touch imprints (60%), 5 FNBs (20%), 3 washings/brushings (12%) and 2 body cavity fluids (8%), from abdomen and pelvis, pelvic and retroperitoneal lymph nodes, ureter, pleura, bone and soft tissue (Table 1).

AGCTs exhibited a range of cytoarchitectural features. Cohesive three-dimensional cell groups (Figure 1A–D) were identified in 19 (76 %) cases, with a ‘streaming’ appearance of cells observed in 7 cases (Figure 1A, 1B), predominantly in FNBs and touch imprints of core biopsies. One ascitic fluid case showed rare, rounded cannon ball-like three-dimensional groups with smooth edges (Figure 1C). Loosely cohesive cell clusters (Figure 1E) and syncytial groups (Figure 1F) of varying size were seen in 11 (44%) and 6 (24%) of cases respectively. Rosette-like or microfollicular structures composed of tumor cells arranged circumferentially around pink hyaline-like material (Figure 1G–I) were present to

varying degrees in 13 cases (52%). Papilliform structures (Figure 1H, 1I) and fragments of metachromatic stroma (Figure 1L) were seen focally in 4 cases (16%) and 3 cases (12%) respectively. Dispersed single cells (Figure 2D) and naked nuclei (Figure 2E) were identified in 23 (92%) and 19 (76%) of cases. Eosinophilic hyaline bodies were seen in 2 cases (1 touch imprint and 1 ascitic fluid) associated with abundant microfollicles and likely represent the denuded hyaline cores of Call-Exner bodies (Figure 2E, 2F). Blood and inflammatory cells (Figure 2F), including hemosiderin-laden macrophages, were present in the background in some cases. Necrosis was identified in one case (Table 1).

Irrespective of cellular arrangement, the tumor cells shared common cytomorphologic features. They predominantly exhibited high nuclear:cytoplasmic (N:C) ratios (n=22; 88%) (Table 1). Nuclear pleomorphism was mild (n=19, 76%) or moderate (n=6, 24%). Nuclei were round to oval, with prominent nuclear grooves (n=25, 100 %), finely granular chromatin (n=23, 92%) and small nucleoli (100%) (Figure 1D, Figure 2A). Irregular nuclear contours were observed in 3 cases (12%). Scant pale cytoplasm was noted in 23 cases (92%) and moderate to abundant cytoplasm (Figure 2B) was seen in 2 cases (8%). Fine cytoplasmic vacuoles (Figure 2 C) were identified focally in 13 cases (52%). Nuclear pseudoinclusions were noted in 2 cases and scattered mitoses were seen in one case (Table 1).

Prior or concurrent histologic material was available for review in 19 of 25 cases, including glass slides and scanned digital images. Multiple growth patterns were identified within each individual tumor in varying proportions (see Table 1 and Figure 3).

Immunocytochemical stains were performed on cell block material in 3 cases. In 9 touch imprint cases, immunohistochemical studies was performed on the corresponding core to confirm the diagnosis of AGCT (Table 4, Figure 2H, 2I). The tumors in this cohort expressed inhibin, FOXL2, SF-1, ER, PR, S100, SMA, WT1, calretinin and desmin. Molecular studies performed on the surgical material using a targeted massively parallel sequencing assay detected the presence of *FOXL2* exon1 p.C134W (c.402C>G) mutations in 7 of 7 AGCT cases tested (100%). Six of the 7 cases (86%) also harbored a *TERT* promoter mutation, variant (g.1295250C>T) or (g.1295228C>T).

Other sex-cord stromal tumors (n=5)

Juvenile granulosa cell tumors (n=2)—Case 1 was a pelvic washing specimen with a single ThinPrep slide. The tumor cells were arranged in loose clusters and single cells and had intermediate N:C ratios, moderate to marked nuclear pleomorphism, round-oval to angulated nuclei, with coarsely granular chromatin, conspicuous nucleoli and fine granular cytoplasm (Figure 4A, 4B). Multinucleated bizarre tumor cells, atypical mitoses and necrosis were also present (Figure 4B–D). The tumor in the concurrent surgical specimen exhibited a solid, diffuse pattern with cytology similar to that seen in the pelvic washing specimen (Figure 4E, 4F) and was designated as JGCT with anaplastic features. Immunohistochemistry on the concurrent surgical specimen showed that the tumor expressed inhibin and FOXL2 (Figure 4G, 4H). DNA sequencing using a targeted massively parallel sequencing assay detected 2 mutations: *AKT1* (NM_001014431) exon4 p.R76_C77insLKTERPRPNTFIIR and *TP53* (NM_000546) exon8 splicing variant p.X293_splice.

Case 2 was an ascitic fluid specimen with ThinPrep and cell block preparations. The tumor cells showed similar cytologic features to those in case 1 but exhibited only moderate nuclear pleomorphism and lacked bizarre tumor cells, atypical mitoses and necrosis. Immunohistochemistry performed on the cell block showed that the tumor cells expressed inhibin and progesterone receptor (Figure 4J, 4K). The surgical specimen showed concordant findings (Figure 4L). No molecular data was available for case 2.

Sertoli-Leydig cell tumor (n=2)—Peritoneal fluid (ThinPrep and cell block preparations) was available in both cases. The tumor cells in both cases were arranged in loose and three-dimensional cell clusters as well as single cells and exhibited intermediate to high N:C ratio, moderate nuclear pleomorphism, round-oval nuclei with moderate nuclear membrane irregularities, coarse chromatin, visible nucleoli and granular-vacuolated cytoplasm (Figure 5A–C). Multinucleated tumor cells were also present in case 2 (Figure 5F). Both cases were categorized as “poorly differentiated SLCT” on prior surgical resection specimens (Figure 10C, 10I). No immunocytochemical or molecular studies were performed on either case.

Steroid cell tumor (n=1)—The cytologic material from the single case of SCT was obtained by FNB of an abdominal nodule. The specimen was highly cellular and the predominant architectural pattern seen was discohesive sheets of cells (Figure 6A–B, 6D–E), with scattered three-dimensional groups (Figure 6F), loose clusters and occasional papillary groups with fibrovascular cores (Figure 6C). The neoplastic cells exhibited low N:C ratio, moderate nuclear pleomorphism, round nuclei with coarsely granular chromatin, multiple small nucleoli, abundant granular-foamy cytoplasm and distinct cytoplasmic borders (Figure 6A–G). Binucleated cells were present and scattered mitoses were also seen (Figure 6B, 6D). Immunocytochemical stains were not performed on this case to establish the cytologic diagnosis. However, calretinin was positive in the surgical specimen (Figure 6I). Molecular data was not available for this case.

DISCUSSION

SCSTs can display a diverse spectrum of clinical and pathologic features. They arise from the primitive sex cords or gonadal stroma and are subdivided into three sub-groups: pure sex cord tumors, pure stromal tumors and mixed sex cord-stromal tumors. The entities in these subgroups can occur in both children and adults and are often associated with ovarian steroid hormone production, leading to various hormone-mediated manifestations[1]. In this study, we evaluated the cytologic features of pure sex cord tumors (AGCT and JCT), a mixed sex cord-stromal tumor (PD-SLCT) and a pure stromal tumor (steroid cell tumor) and correlated the findings with their histologic, immunophenotypic and molecular features.

Gynecologic AGCTs present at stage I in over 90% of cases,[7, 12] of which some may be associated with malignant cells in peritoneal washings due to intraoperative spill, pre-surgical tumor rupture or malignant ascites (stage IC). The overall 5-year survival for early-stage disease is 85–95%, but 15–20% of these patients will have recurrent disease with uncertain long-term prognosis[7]. Higher disease stage at presentation, including direct abdominopelvic extension and metastasis to retroperitoneal lymph nodes and distant sites is

less common. In our cohort, 82% of the patients with recurrent tumors were initially staged as FIGO I-II and the average time to first recurrence was 7.5 years, similar to previously reported findings[23]. Given the propensity of AGCTs to recur in the abdominal cavity and to metastasize to sites amenable to FNB, cytology can be particularly useful as a first-line diagnostic modality.

Twenty of 25 (80%) AGCT specimens in our study were obtained by FNB or touch imprint of a core biopsy and were relatively cellular specimens. The remaining specimens included 3 washings/brushing and 2 body fluids. The most common tumor cell arrangements were in three-dimensional groups, loose clusters, rosettes and singly dispersed. The tumor cells were small or medium-sized with monomorphic round-oval nuclei, high N:C ratio, fine granular chromatin, small nucleoli and prominent longitudinal nuclear grooves. Rare nuclear inclusions were seen in 2 cases and occasional mitoses and focal necrosis in one case. The nuclear features of AGCTs were identified in all specimen types and were best appreciated on Papanicolaou and ThinPrep preparations. Papilliform groups, metachromatic stroma and streaming effect were present in primarily FNB and touch imprint specimens. Round cannonball-like three-dimensional groups were only seen in one ascitic fluid case. Fine cytoplasmic vacuoles were focally seen, primarily in DiffQuik preparations in 52% of cases. Rare cases (8%) exhibited lower N:C ratio with fewer nuclear grooves and more abundant pale or finely vacuolated cytoplasm. Naked nuclei were appreciated only FNB and touch imprint specimens and not in fluids and washings. Eosinophilic hyaline bodies were present in one touch imprint and one ascitic fluid specimen respectively, each of which also exhibited prominent rosette/microfollicular cytoarchitecture.

A previous study[6] of 10 FNB cases described AGCT having large and small overlapping clusters, single cells, prominent metachromatic stroma, naked nuclei and Call-Exner bodies (70%), findings that were confirmed in our study. Prominent blood vessels with perivascular tumor were demonstrated in 10% of their cases[6], while we identified similar vascular papilliform structures in 14% of our cases (Figure 1J, 1K). Papilliform structures seen in our study and other prior reports likely correspond to the pseudopapillary architecture seen in the concurrent histologic specimens (Figure 3D). Pseudopapillary architecture has been previously described in AGCTs as a distinct architectural pattern as a result of discohesion and cellular degeneration around stroma or prominent vessels in tumors with a cystic component.[24] Individual tumor cells were described as monotonous and polygonal with high N:C ratio, central nuclei and nuclear grooves (90%)[6], cytologic features which were also seen in 88%, 100% and 100% of cases respectively in our cohort. A report of 8 metastatic AGCTs[25] noted similar architectural features but in the majority of cases the neoplastic cells had more abundant and vacuolated cytoplasm, prominent central nucleoli and fewer nuclear grooves, the latter seen in only 2 of 8 cases. Another case report also described monomorphic tumor cells with oval coffee bean nuclei, small nucleoli, Call Exner bodies and hemosiderin-laden macrophages in the background[21]. Streaming in three-dimensional clusters and rare eosinophilic hyaline bodies, described in our study, was not reported in any of these studies.

The cytologic features of AGCTs have also been documented in body fluid specimens. Gupta et al[19] described one AGCT case in peritoneal fluid showing three-dimensional

clusters with smooth borders and globular to papillary configuration, Call-Exner bodies and tumor cells with moderate nuclear pleomorphism, vesicular chromatin, conspicuous nucleoli and longitudinal nuclear grooves. Omori et al[22] described two cases, one showing the typical cytoarchitectural features described in our and prior studies and another showing three-dimensional clusters with scalloped borders and round to oval cells with fine chromatin and only occasional longitudinal nuclear grooves. In the body fluid and washing specimens in our cohort, we similarly observed three-dimensional groups, including rare cannon ball-like three-dimensional clusters with smooth edges, microfollicles and singly dispersed cells with comparable cytomorphology. However, we noted no papilliform structures. Additionally, we found eosinophilic hyaline bodies, which appear pale green-blue on ThinPrep (Figure 2F) and were not mentioned in prior reports.

Distinctive cytologic features common to our and previous studies include streaming in three-dimensional cell groups, microfollicular structures, eosinophilic hyaline globules and the presence of longitudinal nuclear grooves in tumor cells, which, in the appropriate clinical setting, are highly suggestive of AGCT. Other cytomorphologic features and architectural patterns, including papilliform groups, are not specific and may be seen in other SCSTs or in epithelial tumors, thus precluding a definitive diagnosis of AGCT based cytomorphology and cytoarchitecture alone. While distinctive cytologic features (microfollicular structures and nuclear grooves) and morphologic comparison with prior (including surgical) specimens are helpful in morphologic diagnosis, definitive diagnosis will often require correlation with the clinical findings, allied with supportive immunocytochemical and molecular evidence. Inhibin A, SF-1, calretinin and FOXL2 are highly sensitive immunohistochemical markers for AGCT, each with a diagnostic sensitivity of greater than 90%[2, 14, 17, 26], with calretinin being the least specific for SCST differentiation[27]. Other immunohistochemical markers which have been reported to be variably positive in AGCTs include WT1, CD99, ER, PR, AE1/AE3, CAM5.2, SMA, S100 and desmin[13]. CD56 has also been shown to be positive to some degree in AGCTs[28]. PAX8, CK7 and EMA are typically negative in these tumors. However, none of the immunochemical markers are useful in distinguishing AGCTs from other SCSTs.

Although immunochemical expression of FOXL2 is somewhat promiscuous among all types of SCST, the *FOXL2* p.C134W somatic missense mutation is highly specific for AGCTs[16, 29] and has been demonstrated in 70%–100% of these tumors;[15, 30–32] this range is likely due to the misdiagnosis of other SCSTs as AGCT on histology[33]. Of the 7 patients with AGCT in our study who had molecular testing performed on prior surgical material, *FOXL2* mutation was detected in all cases. Of these, 6 showed concurrent *TERT* promoter mutations including 4 cases with C228T and 2 cases with C250T variants. Synchronous *TERT* promoter mutations have been widely reported in AGCTs and appear to be associated with adverse prognosis; studies have shown that showed that *TERT* promoter mutations are more frequent in recurrent AGCTs than in primary AGCTs[30, 34]. *KMT2A* inactivating mutations have been reported in 11%–13% of AGCTs[30, 35]. While one study[35] suggested a correlation between the presence of inactivating mutations in *KMT2A* and tumor recurrence, another study[30] reported a similar frequency of these mutations in both primary and recurrent tumors. An inactivating mutation in *KMT2D* (MLL2) (NM_003482) exon10 p.S744* (c.2231C>A) was present in 1 of 7 AGCTs in our study, which was a recurrent

tumor. The *KMT2A* status of the primary tumor in this patient is not known. A different mutation *MLL2* (NM_003482) exon41 p.V4585fs (c.13754delT) was also identified in the recurrent tumor of a second patient in our cohort, the significance of which is unclear.

JGCTs are very rare pure sex-cord tumors which constitute 5% of all granulosa cell tumors[36] and usually occur in the pediatric age group (mean age 13 years), with 90% of cases occurring before 30 years of age[37]. The clinical manifestations are similar to those seen in AGCT patients, with abdominal pain and menstrual disturbances. Prepubertal females often present with precocious pseudopuberty due to estrogen excess. Androgenic manifestations are rare but can occur in a small subset of patients. Tumors confined to the ovary have an excellent prognosis comparable to low-stage AGCT, with a postoperative 5-year disease-free survival rate of >90%[38]. Histologically, JGCTs display a nodular to diffuse architecture with interspersed abortive follicles. The tumor cells have round vesicular nuclei with prominent nucleoli, which lack nuclear grooves and ample pale to eosinophilic cytoplasm. Rare studies have studied the cytologic features of JGCTs and they report more hyperchromatic nuclei and greater nuclear pleomorphism and absence of nuclear grooves and microfollicles in JGCTs when compared to AGCTs[39]. In our study, we examined two peritoneal washing cases which showed similar findings. In comparison to AGCTs, JGCTs exhibited small clusters and singly dispersed round-oval cells, with moderated to marked nuclear pleomorphism, vesicular to coarsely granular chromatin, nuclear hyperchromasia and moderate amounts of pale cytoplasm; they lacked nuclear grooves and rosettes/microfollicles. Both our cases had a concurrent histologic diagnosis of JGCT. In case 1, the tumor exhibited marked nuclear pleomorphism with bizarre multinucleated giant tumor cells, atypical mitoses and necrosis, findings which were also present in the histologic specimen. The tumor in the concurrent surgical specimen expressed both inhibin and FOXL2. Case 2 showed scattered singly dispersed tumor cells and loose clusters of atypical cells with round-oval nuclei, irregular nuclear contours, coarse chromatin, conspicuous nucleoli and moderate pale cytoplasm. Occasional binucleated tumor cells were also seen but no bizarre cells, atypical mitoses or necrosis were observed. Inhibin A and progesterone receptor performed on the cell block supported the diagnosis. The immunohistochemical profile of JGCTs is similar to that of AGCTs and currently there is no marker that can distinguish between the two GCT subtypes. One study reported EMA immunoreactivity in JCTs[40], a feature not usually seen in AGCTs. Given that a small percentage of AGCTs can lack or show only rare nuclear grooves (8% of AGCTs in our study), distinguishing JCTs from AGCTs can be challenging particularly in paucicellular cytologic specimens and in cases in which there is no prior material for comparison. Although JCTs often express FOXL2 by immunochemistry, they do not harbor the canonical *FOXL2* p.C134W mutation seen in virtually all AGCTs. *AKT1* duplications have been reported in 10 of 16 JGCTs[41]. An *AKT1* exon 4 duplication was seen in one of our cases.

SLCTs account for 0.1–0.5% of all ovarian tumors and has a median age at presentation of 28 years[42, 43]. These tumors can present with androgenic manifestations in up to 60% of cases[43]. Three molecular subtypes of SLCT with distinct clinicopathologic features have been described: *DICER1*-mutant (44%, young, androgenic symptoms, moderately to poorly differentiated, retiform or heterologous elements); *FOXL2*-mutant (19%, postmenopausal, abnormal uterine bleeding, moderately or poorly differentiated without heterologous

elements or retiform pattern); and *DICER1*/*FOXL2* wildtype (37%, including all well differentiated tumors)[44]. Moderately and poorly differentiated SLCTs show morphologic overlap with AGCTs and are more likely to recur in the abdomen than well differentiated SLCTs. A few case reports have described the features of poorly[45] and moderately[46] differentiated ovarian SLCTs in cytologic specimens, which showed clusters and singly dispersed round-oval monomorphic cells with vacuolated cytoplasm, prominent nucleoli and rare nuclear grooves, as well as metachromatic globular material surrounded by similar appearing cells (microfollicles)[46]. Another case report[42] described clusters and scattered cells with hyperchromatic nuclei, prominent nucleoli and abundant vacuolated cytoplasm and a separate population of oval to spindled cells with moderate cytoplasm. The cytologic features of retiform SLCT in peritoneal washings have also been previously described in a case report,[47] which described predominantly small ball-like and papillary fragments and small clusters composed of tightly packed small cells, with round to oval hyperchromatic nuclei, inconspicuous nucleoli and scant cytoplasm, along with rare round-oval structures comprised of hyalinized stroma surrounded by a single layer of tumor cells. These structures are somewhat reminiscent of the microfollicles or Call Exner bodies commonly seen in AGCTs. In both of our poorly differentiated SLCTs, some tumor cells exhibited irregular nuclear contours, but lacked longitudinal nuclear grooves, spindled morphology or microfollicular structures as described in other studies.

Steroid cell tumors of the ovary are exceedingly rare, constituting < 0.1 % of ovarian neoplasms[48]. They are pure stromal tumors, which present with androgenic symptoms in more than half of patients and the average age of presentation is 43 years[49]. To the best of our knowledge, the cytologic features of steroid cell tumors has not been previously described. The tumor in our study exhibited predominantly discohesive sheets and loose clusters of large polygonal cells with low N:C ratio, round nuclei, moderate nuclear pleomorphism, coarse chromatin, conspicuous nucleoli and abundant granular-foamy cytoplasm with distinct cytoplasmic borders. Binucleation and scattered mitoses were also seen. These morphologic features correlated well with the corresponding histologic specimen. These tumors are immunoreactive for inhibin, calretinin and Melan-A, but usually do not express FOXL2. FOXL2 expression can be useful in differentiating these tumors from AGCTs with prominent luteinization.

Other differential diagnostic considerations of AGCTs include uterine tumor resembling ovarian sex cord tumor (UTROSCT), Brenner tumor, sex cord tumor with annular tubules (SCTAT), struma ovarii with papillary thyroid carcinoma (PTC), mesothelioma and reactive mesothelial proliferations. UTROSCTs account for less than 0.5% of uterine tumors and though they generally display benign behavior, they have been known for recur[50]. They can exhibit some morphologic and immunophenotypic similarities with ovarian sex cord tumors and which may present a diagnostic challenge if encountered in cytologic specimens. Although they can express sex cord markers including SF-1 and FOXL2[51], they are also usually positive for epithelial and smooth muscle antigens and harbor *NCOA1/NCOA2/NCOA3* rearrangements in 81% of cases[52]. Brenner tumors have been reported to show some cytomorphologic overlap with AGCTs, including round to oval cells with frequent nuclear grooves[53], but they usually express p63 and GATA3[54, 55] and are negative for SCST markers[56]. SCTAT exhibits ring-like tubular structures similar to Call-Exner bodies

in AGCTs but they are commonly seen in patients with Peutz-Jeghers syndrome[8, 57] and harbor *STK11* mutations[57]. Papillary thyroid carcinoma can arise within struma ovarii and will show, in addition to nuclear grooves, other characteristic nuclear features including nuclear clearing and overlapping nuclei[58]. They are also usually positive for thyroid-specific markers[58, 59] and harbor *BRAF* mutations[60]. With peritoneal mesotheliomas, there is usually a clinical finding of extensive peritoneal disease. These tumors can display a range of morphological appearances in cytology specimens, including three-dimensional groups and tubulo-papillary structures, with tumor cells of varying size, nuclear pleomorphism, prominent nucleoli and nuclear membrane irregularities including grooves[61]. These tumors do not express inhibin, FOXL2 or SF-1 and show loss of BAP1 expression in up to 57% and *BAP1* gene alterations in >70% of cases in one report[62]. Several other entities may need to be excluded in a cytology specimen of a patient with current or prior history of an ovarian mass, including other ovarian surface epithelial tumors, ovarian carcinoid tumor and Wilms tumor, particularly in paucicellular specimens. Judicious use of a concise immunohistochemical (and/or molecular) panel and thorough review of clinical and radiological findings can aid correct diagnosis.

The rarity of SCSTs, particularly in cytologic specimens, makes for difficult interpretation even by experienced cytopathologists. AGCTs are the most common SCSTs and are characterized by the presence of 3-dimensional cell groups, some with streaming effect, small loose clusters, rosettes and rare papillae and singly dispersed cells with often high N:C ratio, round-oval nuclei, finely granular chromatin and longitudinal nuclear grooves. Other SCSTs exhibit rare or absent rosettes and nuclear grooves and showed generally lower N:C ratios, greater nuclear pleomorphism, coarse chromatin and more frequently vacuolated cytoplasm. These cytomorphologic features in combination with use of a panel of immunohistochemical markers can allow correct interpretation in the appropriate clinico-radiographic context. Additionally, some SCSTs harbor distinct genetic alterations which can further aid accurate classification.

Funding:

This study was funded in part through the NIH/NCI Cancer Center Support Grant P30 CA008748.

REFERENCES

1. Horta M, Cunha TM. Sex cord-stromal tumors of the ovary: a comprehensive review and update for radiologists. Diagn Interv Radiol. Jul-Aug 2015;21(4):277–86. doi:10.5152/dir.2015.34414 [PubMed: 26054417]
2. Lim D, Oliva E. Ovarian sex cord-stromal tumours: an update in recent molecular advances. Pathology. 2018;50(2):178–189. doi:10.1016/j.pathol.2017.10.008 [PubMed: 29275930]
3. Young RH. Ovarian sex cord-stromal tumours and their mimics. Pathology. Jan 2018;50(1):5–15. doi:10.1016/j.pathol.2017.09.007 [PubMed: 29132723]
4. Babarović E, Franin I, Klarić M, et al. Adult Granulosa Cell Tumors of the Ovary: A Retrospective Study of 36 FIGO Stage I Cases with Emphasis on Prognostic Pathohistological Features. Anal Cell Pathol (Amst). 2018;2018:9148124. doi:10.1155/2018/9148124 [PubMed: 30186737]
5. Atilgan AO, Tepeoglu M, Ozen O, Bilezikçi B. Peritoneal washing cytology in an adult granulosa cell tumor: A case report and review of literature. J Cytol. Jan 2013;30(1):74–7. doi:10.4103/0970-9371.107528 [PubMed: 23661950]

6. Ali S, Gattuso P, Howard A, Mosunjac MB, Siddiqui MT. Adult granulosa cell tumor of the ovary: fine-needle-aspiration cytology of 10 cases and review of literature. Diagn Cytopathol. May 2008;36(5):297–302. doi:10.1002/dc.20798 [PubMed: 18418853]
7. Yasukawa M, Matsuo K, Matsuzaki S, Dainty LA, Sugarbaker PH. Management of recurrent granulosa cell tumor of the ovary: Contemporary literature review and a proposal of hyperthermic intraperitoneal chemotherapy as novel therapeutic option. Journal of Obstetrics and Gynaecology Research. 2021;47(1):44–51. doi:10.1111/jog.14494 [PubMed: 33103312]
8. Young RH. Ovarian Sex Cord-Stromal Tumors: Reflections on a 40-Year Experience With a Fascinating Group of Tumors, Including Comments on the Seminal Observations of Robert E. Scully, MD. Arch Pathol Lab Med. Dec 2018;142(12):1459–1484. doi:10.5858/arpa.2018-0291-RA [PubMed: 30500284]
9. Harbhajanka A, Lamzabi I, Jain R, Syed S, Murro D, Gattuso P. Fine needle aspiration cytology of cystic primary adult granulosa cell tumor of the ovary: Potential diagnostic pitfalls with other cystic ovarian lesions. Diagn Cytopathol Jun 2016;44(6):461–5. doi:10.1002/dc.23458 [PubMed: 26956549]
10. Ottolina J, Ferrandina G, Gadducci A, et al. Is the endometrial evaluation routinely required in patients with adult granulosa cell tumors of the ovary? Gynecol Oncol. Feb 2015;136(2):230–4. doi:10.1016/j.ygyno.2014.12.016 [PubMed: 25527364]
11. Lee IH, Choi CH, Hong DG, et al. Clinicopathologic characteristics of granulosa cell tumors of the ovary: a multicenter retrospective study. J Gynecol Oncol. Sep 2011;22(3):188–95. doi:10.3802/jgo.2011.22.3.188 [PubMed: 21998762]
12. Sakr S, Abdulfatah E, Thomas S, et al. Granulosa Cell Tumors: Novel Predictors of Recurrence in Early-stage Patients. Int J Gynecol Pathol. May 2017;36(3):240–252. doi:10.1097/PGP.0000000000000325 [PubMed: 28727617]
13. Deavers MT, Malpica A, Liu J, Broaddus R, Silva EG. Ovarian Sex Cord-Stromal Tumors: An Immunohistochemical Study Including a Comparison of Calretinin and Inhibin.
14. Al-Agha OM, Huwait HF, Chow C, et al. FOXL2 is a sensitive and specific marker for sex cord-stromal tumors of the ovary. Am J Surg Pathol. Apr 2011;35(4):484–94. doi:10.1097/PAS.0b013e31820a406c [PubMed: 21378549]
15. Jamieson S, Butzow R, Andersson N, et al. The FOXL2 C134W mutation is characteristic of adult granulosa cell tumors of the ovary. Mod Pathol. Nov 2010;23(11):1477–85. doi:10.1038/modpathol.2010.145 [PubMed: 20693978]
16. Carles A, Trigo-Gonzalez G, Cao Q, et al. The Pathognomonic FOXL2 C134W Mutation Alters DNA-Binding Specificity. Cancer Res. Sep 1 2020;80(17):3480–3491. doi:10.1158/0008-5472.CAN-20-0104 [PubMed: 32641414]
17. McCluggage WG. Value of inhibin staining in gynecological pathology. Int J Gynecol Pathol. Jan 2001;20(1):79–85. doi:10.1097/00004347-200101000-00007 [PubMed: 11192074]
18. Deb P, Malik A, Sinha KK. Intraoperative scrape cytology: Adult granulosa cell tumor of ovary. J Cytol. Oct 2011;28(4):207–9. doi:10.4103/0970-9371.86350 [PubMed: 22090698]
19. Gupta N, Rajwanshi A, Dey P, Suri V. Adult granulosa cell tumor presenting as metastases to the pleural and peritoneal cavity. Diagn Cytopathol. Oct 2012;40(10):912–5. doi:10.1002/dc.21675 [PubMed: 21618710]
20. Sun L, Shen YM, Wu XL. [Peritoneal washing cytology in adult granulosa cell tumor: report of a case]. Zhonghua Bing Li Xue Za Zhi. May 8 2018;47(5):378–379. doi:10.3760/cma.j.issn.0529-5807.2018.05.014 [PubMed: 29783808]
21. Ylagan LR, Middleton WD, Dehner LP. Fine-needle aspiration cytology of recurrent granulosa cell tumor: Case report with differential diagnosis and immunocytochemistry. Diagnostic Cytopathology. 2002;27(1):38–41. doi:10.1002/dc.10134 [PubMed: 12112814]
22. Omori M, Kondo T, Yuminamochi T, et al. Cytologic features of ovarian granulosa cell tumors in pleural and ascitic fluids. Diagn Cytopathol. Jul 2015;43(7):581–4. doi:10.1002/dc.23248 [PubMed: 25605680]
23. Zhao D, Zhang Y, Ou Z, Zhang R, Zheng S, Li B. Characteristics and treatment results of recurrence in adult-type granulosa cell tumor of ovary. Journal of Ovarian Research. 2020;13(1)doi:10.1186/s13048-020-00619-6

24. Irving JA, Young RH. Granulosa cell tumors of the ovary with a pseudopapillary pattern: a study of 14 cases of an unusual morphologic variant emphasizing their distinction from transitional cell neoplasms and other papillary ovarian tumors. Am J Surg Pathol. Apr 2008;32(4):581–6. doi:10.1097/PAS.0b013e31815c186f [PubMed: 18301054]
25. Harbhajanka A, Bitterman P, Reddy VB, Park JW, Gattuso P. Cytomorphology and Clinicopathologic Correlation of the Recurrent and Metastatic Adult Granulosa Cell Tumor of the Ovary: A Retrospective Review. Diagn Cytopathol. Dec 2016;44(12):1058–1063. doi:10.1002/dc.23535 [PubMed: 27493080]
26. McCluggage WG, Maxwell P. Immunohistochemical staining for calretinin is useful in the diagnosis of ovarian sex cord-stromal tumours. Histopathology. 2001;38(5):403–408. doi:10.1046/j.1365-2559.2001.01147.x [PubMed: 11422476]
27. Shah VI. Inhibin is more specific than calretinin as an immunohistochemical marker for differentiating sarcomatoid granulosa cell tumour of the ovary from other spindle cell neoplasms. Journal of Clinical Pathology. 2003;56(3):221–224. doi:10.1136/jcp.56.3.221 [PubMed: 12610103]
28. McCluggage WG, McKenna M, McBride HA. CD56 is a sensitive and diagnostically useful immunohistochemical marker of ovarian sex cord-stromal tumors. Int J Gynecol Pathol. Jul 2007;26(3):322–7. doi:10.1097/01.pgp.0000236947.59463.87 [PubMed: 17581419]
29. Kommoss S, Gilks CB, Penzel R, et al. A current perspective on the pathological assessment of FOXL2 in adult-type granulosa cell tumours of the ovary. Histopathology. Feb 2014;64(3):380–8. doi:10.1111/his.12253 [PubMed: 24192202]
30. Pilsworth JA, Cochrane DR, Neilson SJ, et al. Adult-type granulosa cell tumor of the ovary: a FOXL2-centric disease. J Pathol Clin Res. Jan 11 2021;doi:10.1002/cjp2.198
31. Kommoss S, Gilks CB, Penzel R, et al. A current perspective on the pathological assessment ofFOXL2in adult-type granulosa cell tumours of the ovary. Histopathology. 2014;64(3):380–388. doi:10.1111/his.12253 [PubMed: 24192202]
32. D'Angelo E, Mozos A, Nakayama D, et al. Prognostic significance of FOXL2 mutation and mRNA expression in adult and juvenile granulosa cell tumors of the ovary. Mod Pathol. Oct 2011;24(10):1360–7. doi:10.1038/modpathol.2011.95 [PubMed: 21623383]
33. Maillet D, Goulvent T, Rimokh R, et al. Impact of a second opinion using expression and molecular analysis of FOXL2 for sex cord-stromal tumors. A study of the GINECO group & the TMRO network. Gynecol Oncol. Jan 2014;132(1):181–7. doi:10.1016/j.ygyno.2013.10.013 [PubMed: 24157616]
34. Da Cruz Paula A, Da Silva EM, Segura SE, et al. Genomic profiling of primary and recurrent adult granulosa cell tumors of the ovary. Modern Pathology. 2020;33(8):1606–1617. doi:10.1038/s41379-020-0514-3 [PubMed: 32203090]
35. Hillman RT, Celestino J, Terranova C, et al. KMT2D/MLL2 inactivation is associated with recurrence in adult-type granulosa cell tumors of the ovary. Nat Commun. Jun 27 2018;9(1):2496. doi:10.1038/s41467-018-04950-x [PubMed: 29950560]
36. Ye Y, Lv C, Xu S, et al. Juvenile Granulosa Cell Tumors of the Ovary. American Journal of Clinical Pathology. 2020;154(5):635–644. doi:10.1093/ajcp/aqaa081 [PubMed: 32561911]
37. Parikshaa G, Ariba Z, Pranab D, et al. Juvenile granulosa cell tumor of the ovary: A comprehensive clinicopathologic analysis of 15 cases. Ann Diagn Pathol. Feb 10 2021;52:151721. doi:10.1016/j.anndiagpath.2021.151721 [PubMed: 33725665]
38. Bergamini A, Ferrandina G, Candotti G, et al. Stage I juvenile granulosa cell tumors of the ovary: A multicentre analysis from the MITO-9 study. Eur J Surg Oncol. Feb 9 2021;doi:10.1016/j.ejso.2021.02.003
39. Kavuri S, Kulkarni R, Reid-Nicholson M. Granulosa cell tumor of the ovary: cytologic findings. Acta Cytol. Jul-Aug 2010;54(4):551–9. doi:10.1159/000325176 [PubMed: 20715655]
40. McCluggage WG. Immunoreactivity of ovarian juvenile granulosa cell tumours with epithelial membrane antigen. Histopathology. 2005;46(2):235–236. doi:10.1111/j.1365-2559.2004.01989.x [PubMed: 15693901]

41. Auguste A, Bessiere L, Todeschini AL, et al. Molecular analyses of juvenile granulosa cell tumors bearing AKT1 mutations provide insights into tumor biology and therapeutic leads. Hum Mol Genet. Dec 1 2015;24(23):6687–98. doi:10.1093/hmg/ddv373 [PubMed: 26362254]
42. Arora SK, Dey P. Fine needle aspiration cytology of Sertoli-Leydig cell tumors of ovary masquerading as dysgerminoma. Diagn Cytopathol. Jul 2013;41(7):647–9. doi:10.1002/dc.21856 [PubMed: 22102529]
43. Gui T, Cao D, Shen K, et al. A clinicopathological analysis of 40 cases of ovarian Sertoli–Leydig cell tumors. Gynecologic Oncology. 2012;127(2):384–389. doi:10.1016/j.ygyno.2012.07.114 [PubMed: 22850410]
44. Karnezis AN, Wang Y, Keul J, et al. DICER1 and FOXL2 Mutation Status Correlates With Clinicopathologic Features in Ovarian Sertoli-Leydig Cell Tumors. The American Journal of Surgical Pathology. 2019;43(5):628–638. doi:10.1097/pas.0000000000001232 [PubMed: 30986800]
45. Soleimanpour H, Shirian S, Oryan A, Daneshbod K, Bagheri N, Daneshbod Y. Cytologic, immunocytologic, histopathologic and immunohistologic diagnosis of the poorly differentiated sertoli-leydig cell tumor. Acta Cytol. 2011;55(4):382–6. doi:10.1159/000327906 [PubMed: 21791911]
46. Watson B, Siegel CL, Ylagan LR. Metastatic ovarian Sertoli-cell tumor: FNA findings with immunohistochemistry. Diagn Cytopathol. Nov 2003;29(5):283–6. doi:10.1002/dc.10369 [PubMed: 14595797]
47. Guo M, Lim JC, Wojcik EM. Pelvic washing cytology of ovarian Sertoli-Leydig-cell tumor with retiform pattern: a case report. Diagn Cytopathol. Jul 2003;29(1):28–30. doi:10.1002/dc.10301 [PubMed: 12827712]
48. Ismail S, Hraib M, Issa R, Alassi T, Alshehabi Z. A large ovarian steroid cell tumor-not otherwise specified with a unique combination of benign and malignant features as a challenging cause of oligomenorrhea and hirsutism in a 21-year-old Syrian female: a case report. BMC Women's Health. 2021;21(1)doi:10.1186/s12905-021-01244-1
49. Hayes MC, Scully RE. Ovarian steroid cell tumors (not otherwise specified). A clinicopathological analysis of 63 cases. Am J Surg Pathol. Nov 1987;11(11):835–45. doi:10.1097/00000478-198711000-00002 [PubMed: 2823622]
50. Blake EA, Sheridan TB, Wang KL, et al. Clinical characteristics and outcomes of uterine tumors resembling ovarian sex-cord tumors (UTROSCT): a systematic review of literature. Eur J Obstet Gynecol Reprod Biol. Oct 2014;181:163–70. doi:10.1016/j.ejogrb.2014.07.050 [PubMed: 25150955]
51. Croce S, de Kock L, Boshari T, et al. Uterine Tumor Resembling Ovarian Sex Cord Tumor (UTROSCT) Commonly Exhibits Positivity With Sex Cord Markers FOXL2 and SF-1 but Lacks FOXL2 and DICER1 Mutations. Int J Gynecol Pathol. Jul 2016;35(4):301–8. doi:10.1097/PGP.0000000000000240 [PubMed: 26598979]
52. rbpGoebel EA, Hernandez Bonilla S, Dong F, et al. Uterine Tumor Resembling Ovarian Sex Cord Tumor (UTROSCT): A Morphologic and Molecular Study of 26 Cases Confirms Recurrent NCOA1–3 Rearrangement. Am J Surg Pathol. Jan 2020;44(1):30–42. doi:10.1097/pas.0000000000001348 [PubMed: 31464709]
53. Minato J, Tokunaga H, Okamoto S, Shibuya Y, Niikura H, Yaegashi N. Is Imprint Cytology Useful to Diagnose Malignancy for Brenner Tumors? A Case Series at a Single Institute. Acta Cytologica. 2017;61(2):153–159. doi:10.1159/000455997 [PubMed: 28231585]
54. Roma AA, Masand RP. Ovarian Brenner tumors and Walthard nests: a histologic and immunohistochemical study. Hum Pathol. Dec 2014;45(12):2417–22. doi:10.1016/j.humpath.2014.08.003 [PubMed: 25281026]
55. Esheba GE, Longacre TA, Atkins KA, Higgins JP. Expression of the urothelial differentiation markers GATA3 and placental S100 (S100P) in female genital tract transitional cell proliferations. Am J Surg Pathol. Mar 2009;33(3):347–53. doi:10.1097/PAS.0b013e3181908e24 [PubMed: 19092634]
56. Rishi M, Howard LN, Bratthauer GL, Tavassoli FA. Use of monoclonal antibody against human inhibin as a marker for sex cord-stromal tumors of the ovary. Am J Surg Pathol. May 1997;21(5):583–9. doi:10.1097/00000478-199705000-00012 [PubMed: 9158684]

57. Kwon SY, Choe MS, Lee HW, Lee HJ, Shin SJ, Cho CH. Minimal deviation adenocarcinoma of the cervix and tumorlets of sex-cord stromal tumor with annular tubules of the ovary in Peutz-Jeghers syndrome. Journal of Gynecologic Oncology. 2013;24(1):92. doi:10.3802/jgo.2013.24.1.92 [PubMed: 23346318]

58. Al Hassan MS, Saafan T, El Ansari W, et al. The largest reported papillary thyroid carcinoma arising in struma ovarii and metastasis to opposite ovary: case report and review of literature. Thyroid Research. 2018;11(1)doi:10.1186/s13044-018-0054-9

59. Yang CW, Liang WY, Lin JK, Chiou TJ, Lee CH, Jiang JK. Colonic metastasis from a papillary thyroid carcinoma arising in struma ovarii. Int J Colorectal Dis. Jul 2010;25(7):913–4. doi:10.1007/s00384-009-0871-3 [PubMed: 20012969]

60. Garg K, Soslow RA, Rivera M, Tuttle MR, Ghossein RA. Histologically bland "extremely well differentiated" thyroid carcinomas arising in struma ovarii can recur and metastasize. Int J Gynecol Pathol. May 2009;28(3):222–30. doi:10.1097/PGP.0b013e31818a2b99 [PubMed: 19620939]

61. Patel NP, Taylor CA, Levine EA, Trupiano JK, Geisinger KR. Cytomorphologic Features of Primary Peritoneal Mesothelioma in Effusion, Washing, and Fine-Needle Aspiration Biopsy Specimens. American Journal of Clinical Pathology. 2007;128(3):414–422. doi:10.1309/dv1jybl8llyyt4j5 [PubMed: 17709315]

62. Leblay N, Leprêtre F, Le Stang N, et al. BAP1 Is Altered by Copy Number Loss, Mutation, and/or Loss of Protein Expression in More Than 70% of Malignant Peritoneal Mesotheliomas. Journal of Thoracic Oncology. 2017;12(4):724–733. doi:10.1016/j.jtho.2016.12.019 [PubMed: 28034829]

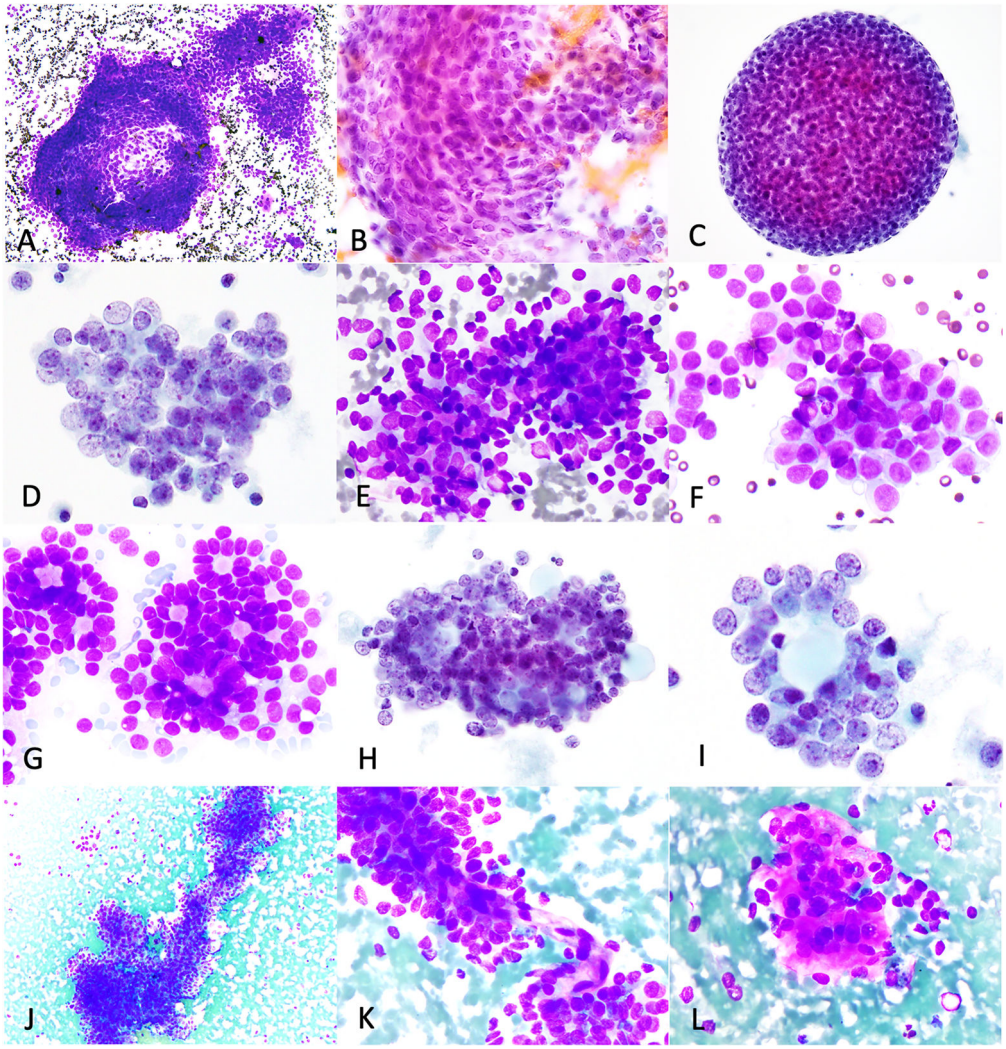

Figure 1: Cytoarchitectural features of adult granulosa cell tumors.

AGCTs exhibited cohesive three-dimensional clusters (A, case 5- abdominal nodule touch imprint, DiffQuik; B, case 2- external iliac lymph node FNB, H&E; C-D, case 15- peritoneal washing, ThinPrep), with streaming (A-B) and rounded contours (C), small loose clusters (E, case 23-retroperitoneal lymph node, touch imprint, DiffQuik), microfollicles/ rosettes (G-I, case 23, DiffQuik and case 15, ThinPrep), papilliform structures (J-K, case 11-pleura, touch imprint, DiffQuik) and cells embedded in metachromatic stroma (L, case 11, DiffQuik).

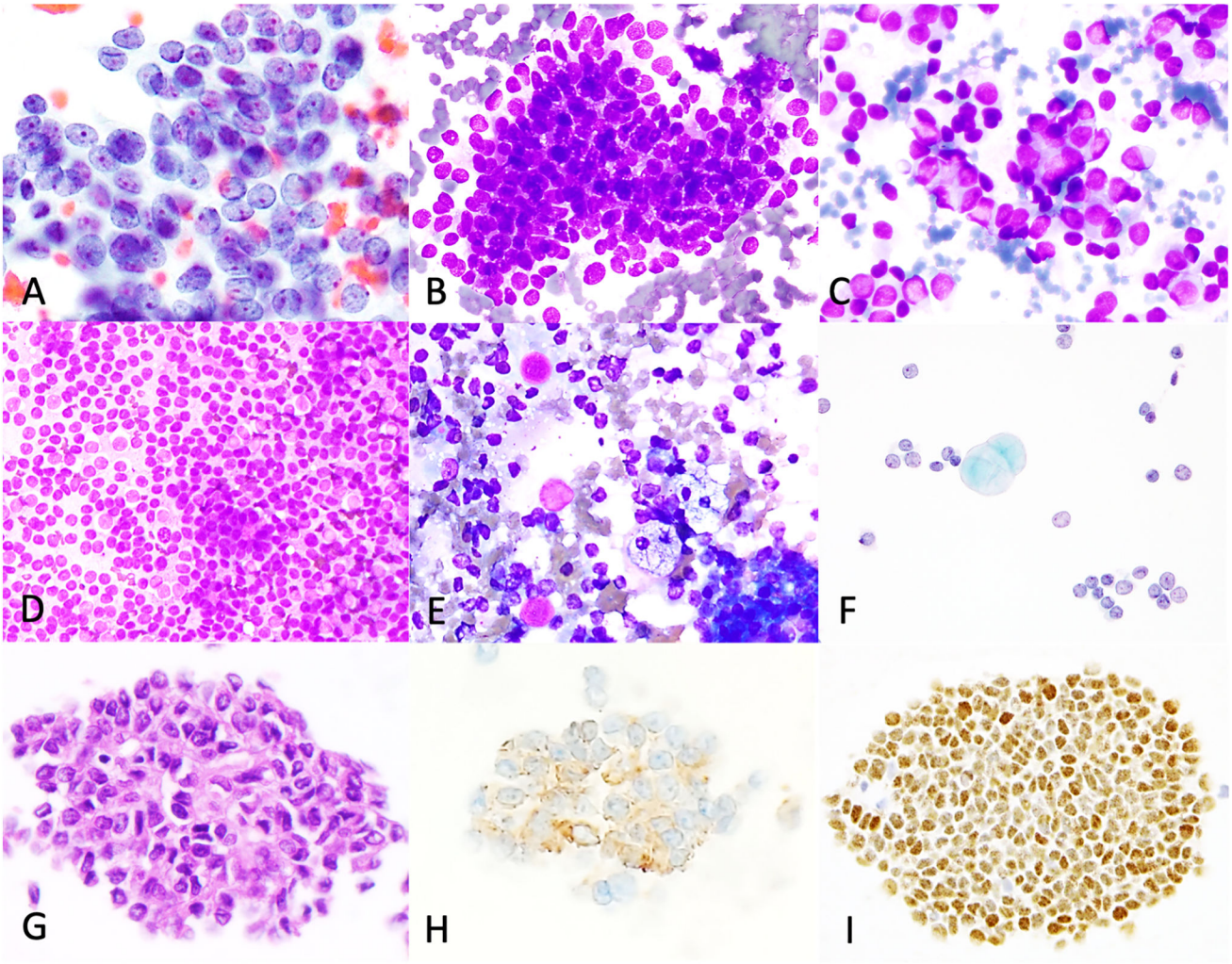

Figure 2: Cytomorphologic and immunophenotypic features of adult granulosa cell tumors.

Individual tumor cells show round to oval nuclei, with longitudinal nuclear grooves, fine granular chromatin, small nucleoli (A, case 17- peritoneum, FNB, Papanicolaou) and scant finely vacuolated cytoplasm (B, case 9- Pelvis, touch imprint, DiffQuik), seen in half of cases. Rare cases show moderate or abundant amounts of cytoplasm (C, case 7- abdominal nodule, FNB, DiffQuik). Single cells, abundant in some cases (D, case 24- peritoneal nodule, touch imprint, DiffQuik), naked nuclei, macrophages and eosinophilic hyaline globules (E-F, case 22- abdomen, touch imprint, DiffQuik, ThinPrep) were present in the background. Immunohistochemical stains performed on cell block (G, case 25- ascitic fluid, H&E) show that the tumor exhibits inhibin (H) and FOXL2 (I) immunoreactivity.

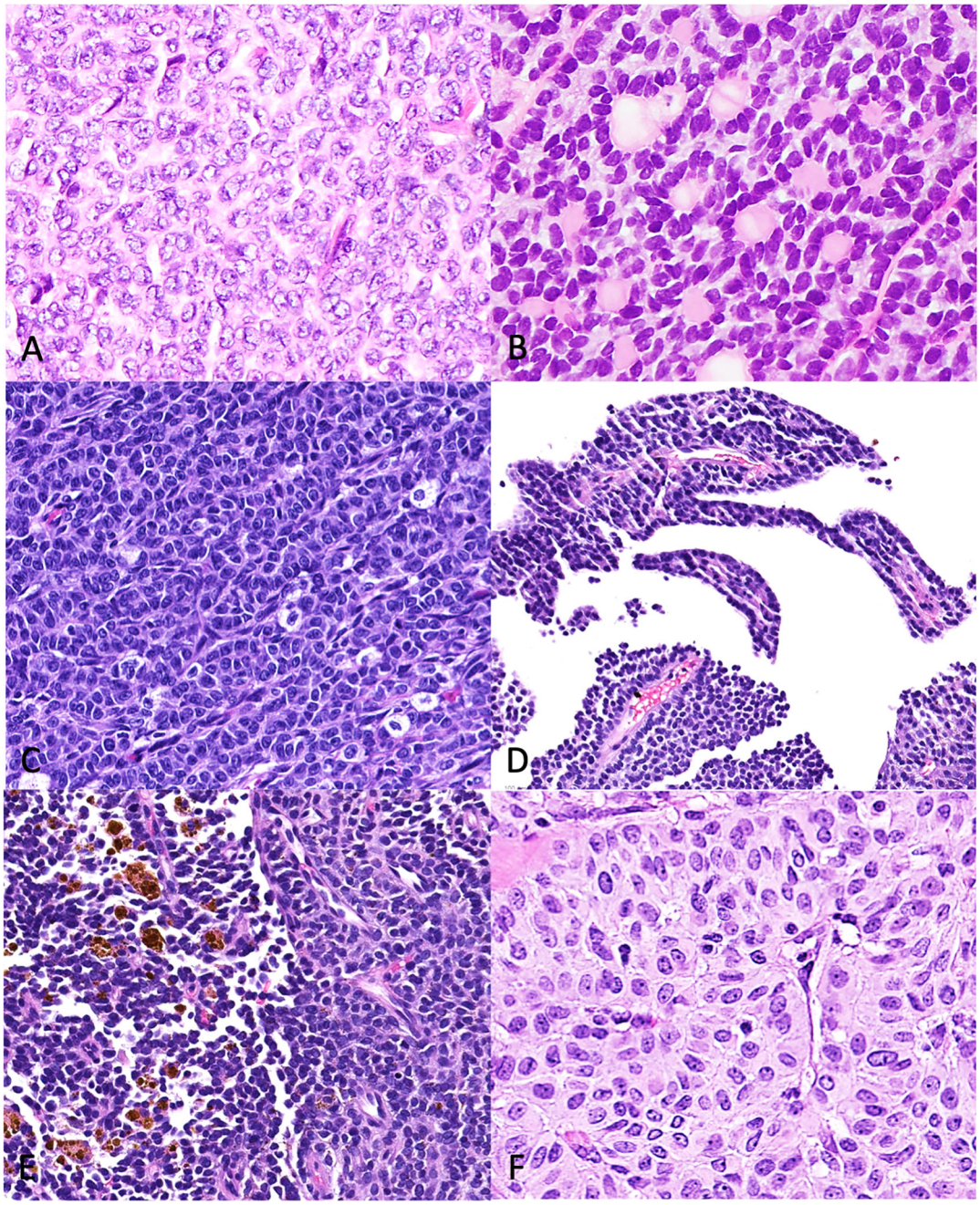

Figure 3: Predominant histologic features of adult granulosa cell tumors in concurrent histology.
Growth patterns present on histology include (A) solid diffuse, (B) Call-Exner-rich/ microfollicular, (C) solid trabecular and pseudo-papillary (D), with hemosiderin-laden macrophages (E) and moderate to abundant cytoplasm (F) in a few cases.

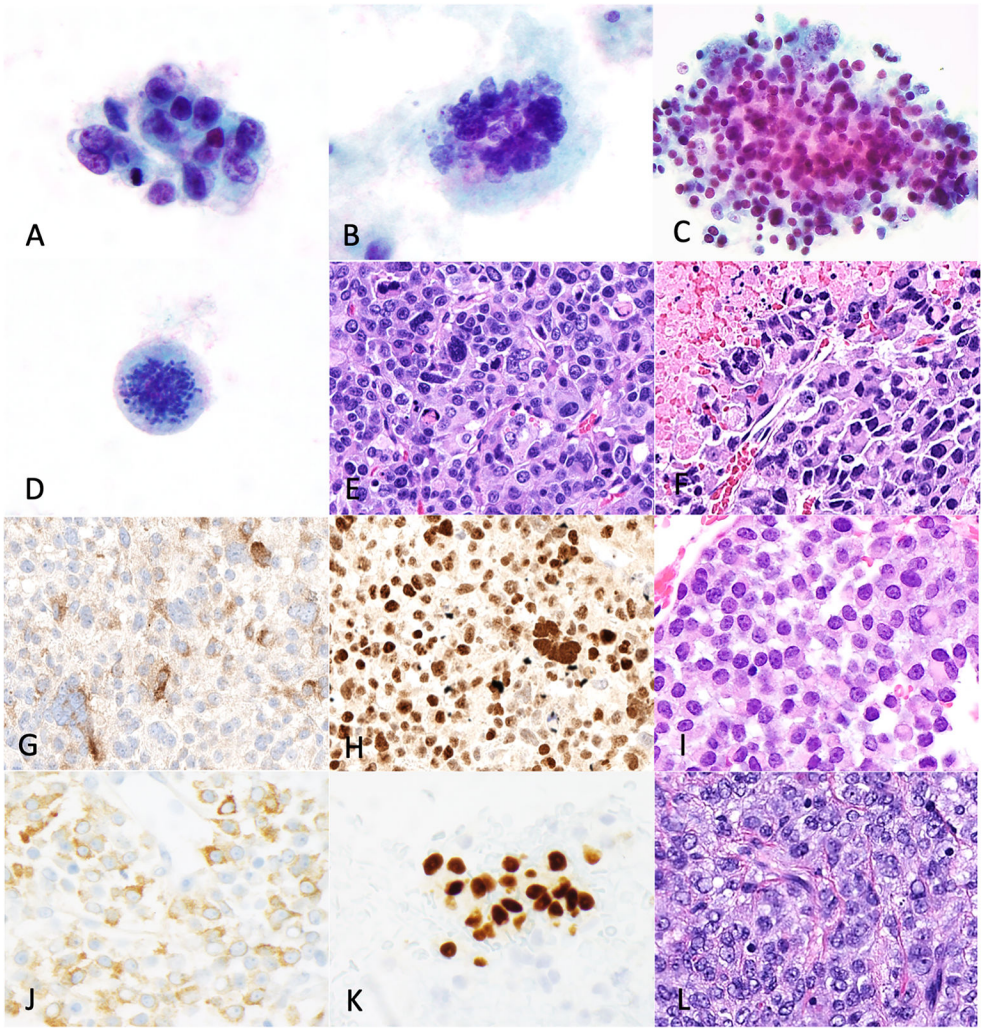

Figure 4: Cytomorphologic features of juvenile granulosa cell tumors

Case 1 (peritoneal washing, Thinprep). Small loose clusters (A) with moderate nuclear pleomorphism, irregular nuclear contours, coarsely granular chromatin, conspicuous nucleoli and fine granular cytoplasm. Multinucleated bizarre tumor cells (B), abundant necrosis (C) and atypical mitoses (D). The corresponding histology (E-F) showed similar finding and expressed inhibin (G) and FOXL2 (H). Case 2 (peritoneal washing, ThinPrep). H&E cellblock (I) shows tumor with similar cytologic features to case 1 and expresses inhibin (J) and PR (K). Solid diffuse-trabecular growth (L) was seen on histology.

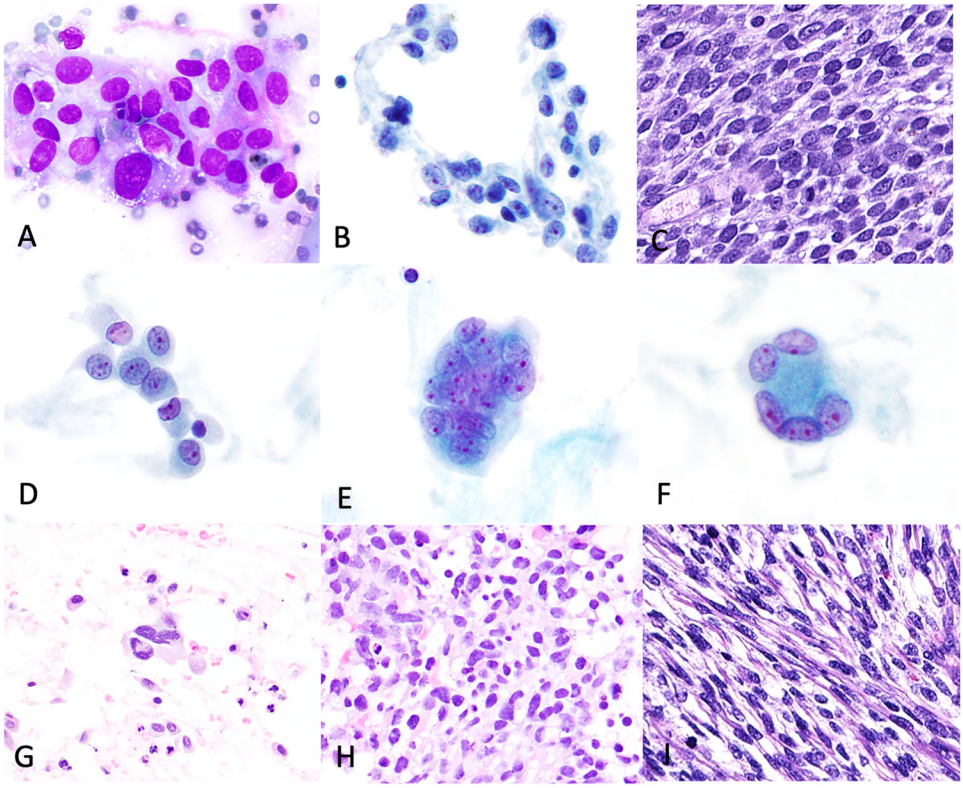

Figure 5: Cytologic features of poorly differentiated Sertoli-Leydig cell tumors

Case 1 (pelvis, touch imprint). Small loose clusters (A, DiffQuik; B, ThinPrep) with intermediate N:C ratio, moderate to marked nuclear pleomorphism, coarse chromatin, conspicuous single-multiple nucleoli and granular to vacuolated cytoplasm. Histology (C) shows a solid diffuse growth pattern. Case 2 (ascitic fluid, ThinPrep, cell block). Single cells and clusters with similar features to case 1 (D-E), but with multinucleated cells (F-G). A Somewhat diffuse, spindled morphology was seen on cell block (H) and corresponding histology (I).

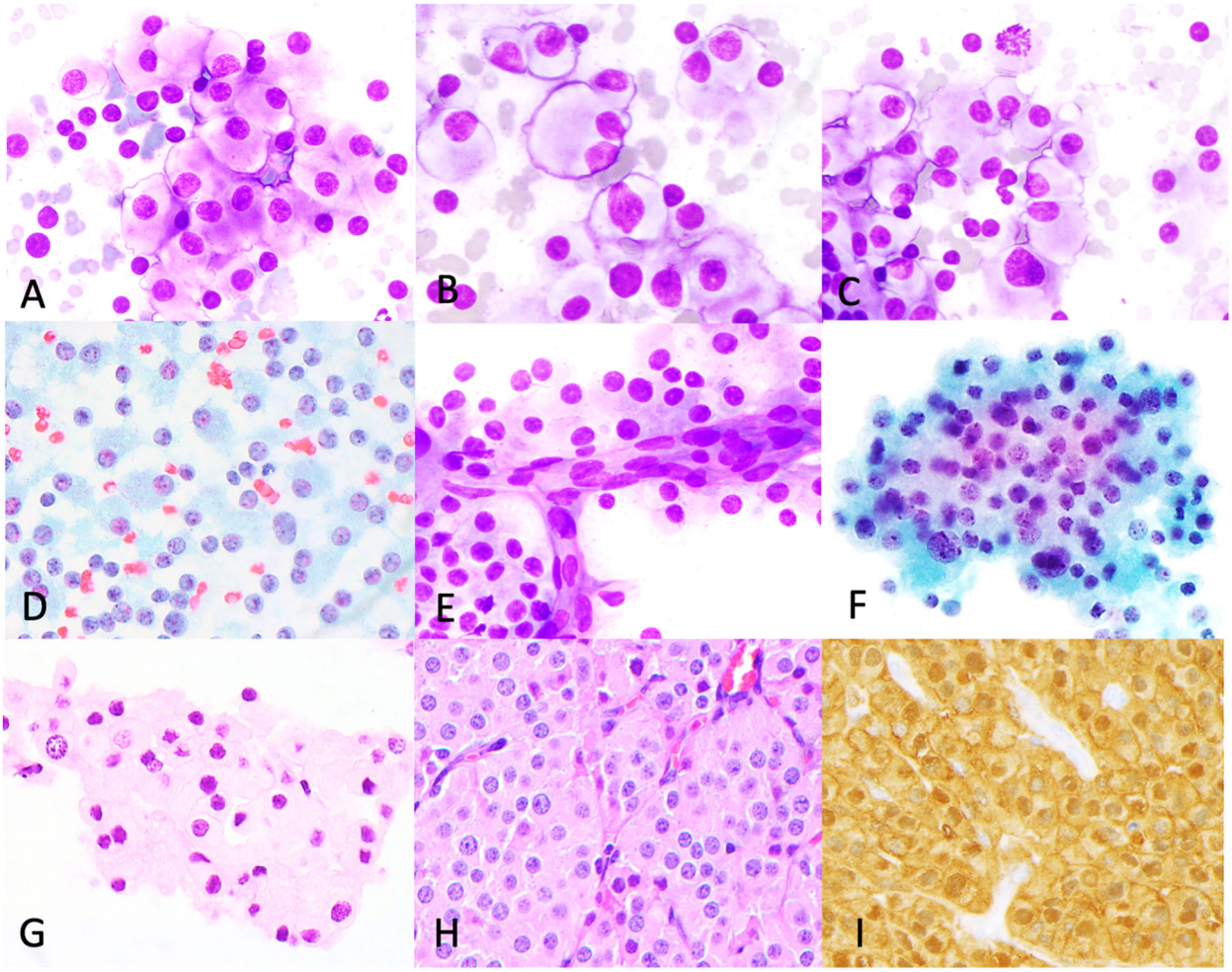

Figure 6: Cytologic features of steroid cell tumor

Steroid cell tumor case (abdominal mass FNB). Dispersed sheets of cells with low N:C ratio, mild nuclear pleomorphism (A-D, DiffQuik, Papanicolaou), binucleation (B), occasional mitoses (C) and rare papillary-like vascular groups (E). three-dimensional groups were also seen (F, ThinPrep). H&E cell block (G) and corresponding histology (H) shows similar features. Tumor in histologic specimen positive for calretinin (I).

Table 1:

Specimen type, site, cytomorphology, histology and molecular features of sex-cord stromal tumors

Patient no. (age at diagnosis[#])	Case No	Specimen site/ type	Cellularity	Cell arrangements[*]	N:C ratio	Nuclear shape	Nuclear grooves	Nuclear pleomorphism	Chromatin pattern	Naked nuclei	Comments	Histologic growth patterns	Mutated genes
Adult granulosa cell tumors													
1 (53 y)	1	Pelvic lymph node (FNB)	I	3D clusters, papillary fragments	H	Oval/ angulated	+	Moderate	Finely granular	−	Scattered cytoplasmic fine vacuoles		
1 (53 y)	2	External iliac lymph node, (FNB)	H	3D clusters with streaming, papillary fragments, stromal fragments, rare rosettes	H	Oval	+	Mild	Finely granular	+			
2 (57 y)	3	Pelvis subcutaneous nodule (FNB)	I	3D clusters with streaming	H	Oval	+	Mild	Finely granular	+	Scattered cytoplasmic fine vacuoles	Solid, diffuse	
2 (57 y)	4	Peritoneum (TI)	I	3D clusters with streaming, rare rosettes	H	Oval	+	Mild	Finely granular	+	Scattered cytoplasmic fine vacuoles	Solid, diffuse, trabecular	
2 (57 y)	5	Abdominal nodule (TI)	H	3D clusters with streaming, rosettes	H	Round/oval	+	Mild	Finely granular	+		Solid, diffuse, vascular, papillary-like areas, HLM	*FOXL2 TERT* KMT2D (MLL)
3 (78 y)	6	Ureter (brushing)	L	3D clusters with streaming	H	Oval	+	Mild	Finely granular	−			*FOXL2 TERT MLL*
4 (74 y)	7	Abdominal nodule (FNB)	H	Large syncytial sheets, 3D clusters and small loose clusters, rare rosettes	H	Round/oval	+	Mild	Finely granular	+	Nuclear inclusions		
5 (59 y)	8	Omental nodule (TI)	H	Large syncytial sheets, small loose clusters, rare rosettes	H	Round/oval	+	Mild	Finely granular	+	Scattered cytoplasmic fine vacuoles	Solid diffuse, nested, pink globules	

Patient no. (age at diagnosis#)	Case No	Specimen site/ type	Cellularity	Cell arrangements*	N:C ratio	Nuclear shape	Nuclear grooves	Nuclear pleomorphism	Chromatin pattern	Naked nuclei	Comments	Histologic growth patterns	Mutated genes
6 (43 y)	9	Pelvis (TI)	H	Large 3D clusters with streaming, rare rosettes	H	Round/oval	+	Mild	Finely granular	+	Scattered cytoplasmic fine vacuoles; nuclear inclusions	Solid, diffuse, HLM	
7 (56 y)	10	Abdomen (TI)	I	3D clusters	H	Round/oval	+, rare	Mild	Finely granular	+		Solid, diffuse	*FOXL2 TERT*
	11	Pleura (TI)	I	Large syncytial sheets, papillary fragments, 3D and loose clusters, rare rosettes, metachromatic stroma	H	Round/oval	+	Mild	Finely granular	+	Scattered cytoplasmic fine vacuoles	Solid, diffuse, papilla-like vascular structures, focal hyaline stroma, rare Call-Exner bodies, HLM	
8 (63 y)	12	Abdomen (TI)	H	3D clusters, small loose clusters	H	Oval	+	Mild	Finely granular	+	Scattered cytoplasmic fine vacuoles		*FOXL2 TERT*
8 (64 y)	13	Abdomen (TI)	H	Large 3D clusters, small loose clusters	H	Round/oval	+	Mild	Vesicular	+	Scattered cytoplasmic fine vacuoles		
9 (90 y)	14	Pelvis (TI)	I	Rare loose clusters; one possible rosette-like structure	H	Oval	+	Mild	Vesicular	+	Scattered cytoplasmic fine vacuoles	Solid, diffuse, trabecular	
10 (54 y)	15	Peritoneal washing	H	Small sheets and 3D clusters, rosettes	H	Round/oval	+	Mild	Finely granular	−	Inflammation	Solid, diffuse, Call-Exner bodies	
11 (26 y)	16	Ascitic fluid	L	Small loose clusters	H	Round/oval/ angulated	+, rare	Moderate	Finely granular	−	Inflammation	Solid, diffuse, nested, abortive follicles, HLM	

Patient no. (age at diagnosis[#])	Case No	Specimen site/ type	Cellularity	Cell arrangements[*]	N:C ratio	Nuclear shape	Nuclear grooves	Nuclear pleomorphism	Chromatin pattern	Naked nuclei	Comments	Histologic growth patterns	Mutated genes
12 (47 y)	17	Peritoneum (FNB)	H	Large syncytial sheets, 3D and small loose clusters, rare rosettes, metachromatic stroma	H	Oval	+	Moderate	Finely granular	+		Solid, diffuse, cords	*FOXL2 TERT*
13 (50 y)	18	Peritoneal washing	L	Small 3D clusters	I-H	Oval/ angulated	+	Moderate	Finely granular	−	Scattered cytoplasmic fine vacuoles	Solid, diffuse, nested	
14 (71 y)	19	Iliac bone (TI)	I	3D clusters	H	Round/oval	+	Moderate	Finely granular	+	Scattered cytoplasmic fine vacuoles; mitoses, necrosis, inflammation	Solid, diffuse, many histiocytes	
14 (71 y)	20	Sacral soft tissue (TI)	I	3D clusters with streaming, small loose clusters, metachromatic stroma	H	Round/oval	+	Moderate	Finely granular	+	Scattered cytoplasmic fine vacuoles	Solid, diffuse	
15 (65 y)	21	Subcutaneous nodule (TI)	I	Small, loose clusters	I	Round/oval	+	Mild	Finely granular	+		Solid, diffuse, hyaline stroma	
16 (66 y)	22	Abdomen (TI)	H	3D clusters, rosettes, eosinophilic hyaline bodies	H	Round/oval	+	Mild	Finely granular	+		Call-Exner bodies, focal solid diffuse	
17 (57 y)	23	Retroperitoneal lymph node (TI)	H	Syncytial sheets, small loose clusters, rosettes; metachromatic stroma	L	Round/oval	+	Mild	Finely granular	+	Scattered cytoplasmic fine vacuoles	Solid, diffuse, rare Call-Exner bodies	*FOXL2 TERT*
18 (66 y)	24	Peritoneal nodule (TI)	H	3D clusters, papillary like structures, rare rosettes	H	Round/oval	+	Mild	Finely granular	+		Solid, diffuse, rare Call-Exner bodies	

Patient no. (age at diagnosis[#])	Case No	Specimen site/ type	Cellularity	Cell arrangements[*]	N:C ratio	Nuclear shape	Nuclear grooves	Nuclear pleomorphism	Chromatin pattern	Naked nuclei	Comments	Histologic growth patterns	Mutated genes
19 (32 y)	25	Ascitic fluid	L	Small, loose clusters, rare eosinophilic hyaline bodies	H	Oval	+	Mild	Finely granular	−		Solid, nested, Call-Exner bodies	*FOXL2*
Juvenile granulosa cell tumors													
20 (7 y)	1	Peritoneal washing	I	Small, loose clusters	I-H	Round/oval; Bizarre and multinucleated cells	−	Marked	Coarsely granular	+	Mitotic figures, including atypical forms	Solid, diffuse, focal fibrous septae, necrosis, eosinophilic globules	*TP53* *AKT1*
21 (66 y)	2	Peritoneal washing	L	Loose clusters	I	Round/oval/ angulated	−	Moderate	Vesicular	−		Solid, diffuse, trabecular	
Poorly differentiated Sertoli-Leydig cell tumors													
22 (22 y)	1	Pelvis (TI)	I	Small 3D and loose clusters	I-H	Oval/ angulated	−	Moderate	Coarsely granular	+		Solid, diffuse	*DICER1* *TERT*
23 (36 y)	2	Ascitic fluid	I	Small clusters	I	Round/oval; Binucleation	−	Mild-moderate	Finely granular	−		Solid, diffuse, spindled	
Steroid cell tumor													
24 (81 y)	1	Abdominal mass (FNB)	H	Sheets, 3D clusters and papillary like structures	L	Round; Binucleation	−	Moderate	Speckled and open/ granular	+	Abundant granular cytoplasm; rare mitotic figures	Solid, diffuse, nested	*GNAS*

[#]- Age at diagnosis of cytologic specimen

3D – three dimensional; TI- touch imprint of core biopsy; FNB- fine needle biopsy; H-high; I- intermediate; L-low; HLM-hemosiderin laden macrophages

[*]singly dispersed tumor cells also seen; + present; − not present

Table 2:

Clinical details of patients with sex cord stromal tumors

Patient	Diagnosis	Age at initial diagnosis (years)	Stage at initial diagnosis	Time to first recurrence (years)
1	AGCT	35	IC2	10.0
2	AGCT	30	IC	8.0
3	AGCT	63	Unknown	5.0
4	AGCT	66	IC	5.0
5	AGCT	47	I	10.0
6	AGCT	33	IC	5.0
7	AGCT	43	IA	3.0
8	AGCT	31	I	12.0
9	AGCT	90	No staging	FOD
10	AGCT	54	II	FOD
11	AGCT	26	IC	LTF
12	AGCT	47	IA	10.0
13	AGCT	42	IC	7.0
14	AGCT	43	II	7.0
15	AGCT	38	Unknown	30.0
16	AGCT	42	II	15.0
17	AGCT	52	IIIC	5.0
18	AGCT	45	I	12.0
19	AGCT	28	IC	5.0
20	JGCT	7	IC2	FOD
21	JGCT	65	IIIB	1.3
22	PD-SLCT	15	IA	6.9
23	PD-SLCT	35	IC2	1.8
24	SCT	80	IA	1.0

AGCT – adult granulosa cell tumor; JGCT – juvenile granulosa cell tumor; PD-SLCT – poorly differentiated Sertoli-Leydig cell tumor; SCT – Steroid cell tumor, not otherwise specified FOD- free of disease; LTF- lost to follow-up

Table 3:

Sites and types of specimen and cytologic preparations

Specimen Site/type	No. of cases (patients)	Cytologic preparations evaluated
Fine needle aspiration biopsies (FNBs)		
Pelvic LNs	2 (1)	DQ, PAP, +/− H&E smears, ThinPrep, CB
Abdomino-pelvic nodules	4 (4)	DQ, PAP, +/− H&E smears, ThinPrep, CB
Total	***6 (5)***	
Touch preparations		
Pleura	1 *	DQ touch imprints, ThinPrep, +/− CB
Subcutaneous/soft tissue	2 **	DQ touch imprints, ThinPrep, +/− CB
Abdomino-pelvic nodules	12 (10)	DQ touch imprints, ThinPrep, +/− CB
Iliac bone	1	DQ touch imprints, ThinPrep, +/− CB
Total	***16 (13)***	
Body fluids		
Ascitic fluid	2 (2)	ThinPrep, CB
Total	***2 (2)***	
Washings/Brushings		
Peritoneal washing	4 (4)	ThinPrep, CB
Ureter brushing	1 (1)	ThinPrep
Total	***5 (5)***	

* One patient had one pleura and one abdomen nodule specimen.

** One patient had one bone and one soft tissue nodule specimen.

DQ – DiffQuik; PAP – Papanicolaou; H&E – hematoxylin & eosin; CB – cell block

Table 4:

Immunophenotypic features of adult granulosa cell tumors

Marker	Clone, Vendor	Cell block material (n=3)			Touch imprint of core biopsy (n=9)		
		# of tested cases	*# of positive cases*	*%*	*# of tested cases*	*# of positive cases*	*%*
Inhibin	R1, Cell Marque	3	3	100	6	6	100
FOXL2	668, Novus	1	1	100	2	2	100
PR	16, Leica	-	-	-	3	3	100
ER	6F11, Leica	-	-	-	5	5	100
SF-1	N1665, Invitrogen	-	-	-	1	1	100
Calretinin	SP65, Ventana	1	0	0	1	0	0
WT1	WT49, Leica	-	-	-	1	1	100
S100	Polyclonal, Dako	-	-	-	3	2	67
SMA	1A4, Cell Marque	-	-	-	2	2	100
Desmin	DE.R.11, Ventana	-	-	-	1	1	100